Cramér-Rao Lower Bounds for Frequency andPhase NDA Estimation From Arbitrary Square QAM-Modulated Signals

Faouzi Bellili, Nesrine Atitallah, Sofiène Affes, *Senior Member, IEEE*, and Alex Stéphenne, *Senior Member, IEEE*

***Abstract*—In this paper, we derive for the first time the analytical expressions of the exact Cramér–Rao lower bounds (CRLBs) of the carrier frequency and the carrier phase from square quadrature amplitude modulated (QAM) signals, assuming the noise power and the signal amplitude to be completely unknown. The signal is assumed to be corrupted by additive white Gaussian noise (AWGN). The main contribution of this paper consists in deriving the analytical expressions for the non-data-aided (NDA) Fisher information matrix (FIM) for higher-order square QAM-modulated signals. We prove that the problem of estimating the synchronization parameters is separable from the one of estimating the signal and the noise powers by showing that the FIM is block diagonal. Besides, we show analytically that the phase CRLB is higher than the frequency CRLB, implying that it is much easier to estimate the frequency than the distortion phase. It will be seen that the CRLBs differ widely from one modulation order to another in the medium SNR range. The newly derived expressions corroborate previous attempts to numerically or empirically compute the considered CRLBs as well as their asymptotical expressions derived only in special SNR regions.**

***Index Terms*—CRLB, MCRLB, NDA estimation, phase and frequency estimation, QAM, synchronization.**

I. Introduction

QUADRATURE amplitude modulation (QAM) is a relevant technique to convey data in modern digital communications. Because the number of its transfer constellation points remains high, it is possible to transmit more bits per every position change. In this context, coherent receivers must in practice compensate for the phase and the frequency offsets introduced by the channel using reliable estimation techniques. These techniques are usually derived assuming the signal amplitude and the noise power to be either perfectly estimated or absolutely known at the receiver. Roughly speaking, they can be mainly categorized into two major categories: data-aided (DA) and non-data-aided (NDA) estimators. In DA estimation, *a priori* known symbols are transmitted to assist the estimation process. However, in the NDA mode, the required parameters are blindly estimated assuming the transmitted symbols to be completely unknown. So far, many DA and NDA phase and frequency estimators [2]–[4] have been reported in the literature where a given unbiased estimator is usually said to outperform another one, over a given SNR range, if it exhibits a lower variance. In this context, it has been extremely useful in practice to determine a common lower bound on the variance of unbiased estimators. This bound serves mainly as a benchmark to evaluate the achievable performance on the estimation of a given parameter.

The Cramér–Rao lower bound (CRLB) meets this requirement and is often used in signal processing. However, due to the mathematical difficulty of the exact CRLB's analytical derivation, several Cramér–Rao like bounds have been proposed such as the asymptotic CRLB (ACRLB) [5], [6] and the modified CRLB (MCRLB) [7]. The ACRLB of the phase and frequency estimates, which refers to the approximate expression for the exact CRLB but only for sufficiently high or low SNR values, was investigated in [5], [6]. The MCRLB is another bound which is simpler to evaluate but looser than the exact (true) CRLB, especially in the low-SNR region. The MCRLB for scalar parameter estimation was firstly introduced and derived for synchronization parameters in [7], where the separate estimation of the carrier frequency, the carrier phase and the time epoch was considered. The MCRLB was extended to vector parameter estimation in [8] where it was derived for the joint estimation of the carrier frequency, the carrier phase and the symbol epoch of a linearly-modulated signal, but assuming the signal amplitude and the noise power to be perfectly known. In practice, however, the latter two parameters are unknown to the receiver and need to be estimated as well.

On the other hand, it is well known that the MCRLB is a good approximation of the exact CRLB only at high SNR levels and that it becomes significantly loose at low and moderate SNRs. Therefore, without the knowledge of the exact CRLB in the latter SNR regions, it is impossible to evaluate and compare the accuracy of a given unbiased NDA estimator with the

Manuscript received December 13, 2009; accepted May 05, 2010. Date of publication May 24, 2010; date of current version August 11, 2010. The associate editor coordinating the review of this manuscript and approving it for publication was Dr. Mark Coates. This work was supported by a Canada Research Chair in Wireless Communications, PROMPT Inc., the Cooperative Research and Development program of NSERC, and Ericsson Canada. This work was accepted for publication in part in IEEE GLOBECOM, Honolulu, Hawaii, November–December, 2009 [1].

F. Bellili and S. Affes are with the INRS-EMT, 800, de la Gauchetière Ouest, Bureau 6900, Montreal, QC H5A 1K6, Canada (e-mail: bellili@emt.inrs.ca; affes@emt.inrs.ca).

N. Atitallah is with the Signals and Systems Department, Tunisia Polytechnic School, and also with the INRS-EMT, 800, de la Gauchetière Ouest, Bureau 6900, Montreal, QC H5A 1K6, Canada (e-mail: atital@emt.inrs.ca).

A. Stéphenne is with Huawei Technologies, Ottawa, ON K2K 3C9, Canada, and also with the INRS-EMT, 800, de la Gauchetière Ouest, Bureau 6900, Montreal, QC H5A 1K6, Canada (e-mail: stephenne@ieee.org).

Color versions of one or more of the figures in this paper are available online at http://ieeexplore.ieee.org.

Digital Object Identifier 10.1109/TSP.2010.2051154

fundamental performance limit. Consequently, several reported works [9], [10] and the references therein dealt with either the empirical/numerical computation or the analytical derivation of the exact CRLB of the synchronization parameters, depending on the SNR region. In fact, for QAM signals, the CRLBs for the joint phase and frequency estimation were numerically computed, from very complex expressions, at low SNR values and empirically evaluated at moderate and high SNRs using Monte Carlo evaluation [9]. For PSK signals, however, using a Taylor series expansion of the log-likelihood function, approximate analytical expressions for the carrier phase and frequency exact CRLBs were derived in [10], but only in the low-SNR regime (i.e., ACRLB). More so, in these two works [9], [10], the noise power and the signal amplitude were also considered as perfectly known. The closed-form expressions of the exact CRLBs pertaining to the joint estimation of the carrier phase, the carrier frequency, the signal amplitude and the noise power were recently derived by Delmas in [11], but only in the particular cases of BPSK/MSK and QPSK transmissions. However, considering higher-order QAM constellations, which are and will be widely used in current and future high-speed communication technologies, there are no closed-form expressions for the exact CRLBs of the carrier phase and frequency offset NDA estimates. Thus, the new contribution embodied by this paper will be the derivation of the analytical expressions for the NDA CRLBs of the considered synchronization parameters from any square QAM waveform over AWGN channels by further assuming the signal amplitude and the noise power to be completely unknown. Our new expressions generalize the elegant expressions recently derived in [11] from the BPSK/MSK and QPSK cases to higher-order square QAM signals. Besides, we prove that we are actually dealing with two disjoint problems regarding the estimation of the carrier frequency and phase offsets, on one hand, and the estimation of the signal amplitude and the noise power on the other hand. The newly derived expressions are of a great value in that they allow to quantify and analyze the achievable performance on the carrier frequency and the carrier phase NDA estimation from square QAM waveforms.

The rest of this paper is organized as follows. In Section II, we introduce the system model that will be adopted throughout the article. In Section III, we derive the closed-form expressions for the different FIM elements and the corresponding NDA CRLBs of any square QAM modulated signals. Some graphical representations of the newly derived expressions and discussions will be presented in Section IV. Finally, concluding remarks will be drawn out in Section V.

II. System Model

Consider a traditional digital communication system broadcasting and receiving any square QAM-modulated signal. The channel is supposed to be of a constant gain coefficient S over the observation interval. We assume a received signal which is AWGN-corrupted with noise power σ^2. Assuming perfect time synchronization, the received signal at the output of the matched filter can be modelled as a complex signal as follows:

$$y(k) = Sa(k)e^{j2\pi k\nu}e^{j\phi} + w(k), \qquad k = k_0, \dots, k_0 + K - 1 \quad (1)$$

where, at time index k, $a(k)$ is the transmitted symbol and $y(k)$ is the corresponding received sample. The noise component $w(k)$ is modelled by a zero-mean complex Gaussian random variable with independent real and imaginary parts, each of variance $\sigma^2/2$. K is the total number of received samples in the observation interval. Moreover, the transmitted symbols are assumed to be independent and equiprobable.[1] The parameters ϕ, ν and S are the deterministic unknown carrier phase, carrier frequency and signal amplitude, respectively. Furthermore, in order to derive standard lower bounds, the constellation energy is supposed to be normalized to one, i.e., $\mathrm{E}\{|a(k)|^2\} = 1$ where $\mathrm{E}\{\cdot\}$ and $|\cdot|$ refer to the statistical expectation of any random variable and the module of any complex number, respectively. Denoting the transpose operator by the superscript T, we define the following unknown parameter vector:

$$\boldsymbol{\theta} = [\nu\ \phi\ S\ \sigma^2]^T. \quad (2)$$

The signal-to-noise ratio (SNR) of the system is defined as

$$\rho = \frac{S^2}{\sigma^2}. \quad (3)$$

We mention that, throughout this paper, X_k denotes any random variable while $x(k)$ denotes its realization. Matrices and vectors will be represented by bold upper and lower case letters, respectively. $\mathrm{E}_Z\{\cdot\}$ and $\mathrm{E}_{(Z_1,Z_2)}\{\cdot\}$ will also refer to the expectation with respect to any univariate random variable Z and any bivariate random variable (Z_1, Z_2), respectively. We will also denote by j the complex number that verifies $j^2 = -1$. Moreover, the operators $\{\cdot\}^*$, $\Re\{\cdot\}$, and $\Im\{\cdot\}$ return the conjugate, the real, and the imaginary parts of any complex number, respectively.

III. Derivation of the Parameters' NDA CRLBs in Square QAM Transmissions

In this section, we derive the analytical expressions of the exact NDA CRLBs of the considered synchronization parameters when the unknown transmitted signal is square QAM-modulated and AWGN-corrupted. This means that the transmitted symbols are assumed to be drawn from any M-ary square QAM constellation, i.e., $M = 2^{2p} (p = 1, 2, 3 \dots)$. As shown in [12], the CRLB for vector parameter estimation is given by

$$\mathrm{CRLB}(\boldsymbol{\theta}) = \boldsymbol{I}^{-1}(\boldsymbol{\theta}) \quad (4)$$

where $\boldsymbol{\theta}$ is defined in (2) and $\boldsymbol{I}(\boldsymbol{\theta})$ is the Fisher information matrix (FIM) whose entries are defined as

$$[\boldsymbol{I}(\boldsymbol{\theta})]_{ij} = -\mathrm{E}_{\boldsymbol{Y}}\left\{\frac{\partial^2 \ln(P[\boldsymbol{y};\boldsymbol{\theta}])}{\partial\theta_i\partial\theta_j}\right\} \quad (5)$$

where $\boldsymbol{Y}$ is the random variable whose realization is $\boldsymbol{y} = [y(k_0), y(k_0+1), \dots, y(k_0+K-1)]^T$ and $P[\boldsymbol{y};\boldsymbol{\theta}]$ is the probability density function (pdf) of $\boldsymbol{y}$ parameterized by $\boldsymbol{\theta}$ when the transmitted symbols are completely unknown (no training sequence). Usually, the derivation of the NDA CRLB involves tedious algebraic manipulations. These mainly consist in the derivation of the FIM elements which are often

[1]Note that, in this paper, we are dealing with stochastic CRLBs since the transmitted sequence is assumed random.

numerically tackled for higher-order modulations. However, in this paper, we are able to derive for the first time their analytical expressions in case of square QAM transmissions providing, thereby, the analytical expressions of the considered NDA CRLBs.

In fact, under the assumptions made so far and for any M-ary QAM constellation (i.e., $M = 2^p$ for arbitrary integer $p \geq 2$), it can be seen that the pdf of the received sample $y(k)$ parameterized by $\boldsymbol{\theta}$ ($P[y(k);\boldsymbol{\theta}]$), in the NDA mode, is given by:

$$P[y(k);\boldsymbol{\theta}] = \frac{1}{M\pi\sigma^2}\exp\left\{-\frac{I(k)^2+Q(k)^2}{\sigma^2}\right\}D_{\boldsymbol{\theta}}(k) \quad (6)$$

where, referring to the constellation alphabet by $\mathcal{C}$, $D_{\boldsymbol{\theta}}(k)$ is given by

$$D_{\boldsymbol{\theta}}(k) = \sum_{c_i\in\mathcal{C}}\exp\left\{-\frac{S^2|c_i|^2}{\sigma^2}\right\} \times \exp\left\{\frac{2S\,\Re\left\{y(k)^* e^{j(2\pi k\nu+\phi)}c_i\right\}}{\sigma^2}\right\}. \quad (7)$$

It is seen for (7) that the major advantage offered by the square QAM constellations is that $P[y(k);\boldsymbol{\theta}]$ can be factorized, making it possible to obtain simpler analytical expressions, as a function of the true SNR, ρ, and the modulation order,[2] p, for the FIM elements given by (5). Indeed, when $M = 2^{2p}$ for any $p \geq 1$, we have $\mathcal{C} = \{\pm(2i-1)d_p \pm j(2m-1)d_p\}_{i,m=1,2,\ldots,2^{p-1}}$ where $2d_p$ is the intersymbol distance in the I/Q plane. Recall that, in order to derive standard CRLBs, the square QAM constellation energy is always supposed to be normalized to one, i.e., $\mathrm{E}\{|a(k)|^2\} = 1$. Therefore, d_p is derived using the following formula:

$$\frac{\sum_{l=1}^{2^{2p}}|c_l|^2}{2^{2p}} = 1 \quad (8)$$

which yields the following result:

$$d_p = \frac{2^{p-1}}{\sqrt{2^p\sum_{l=1}^{2^{p-1}}(2l-1)^2}}. \quad (9)$$

To begin with, we show in Appendix A that $D_{\boldsymbol{\theta}}(k)$ is factorized as follows[3]:

$$D_{\boldsymbol{\theta}}(k) = 4F_{\boldsymbol{\theta}}(u(k)) \times F_{\boldsymbol{\theta}}(v(k)) \quad (10)$$

where $u(k)$ and $v(k)$ are defined as

$$\begin{aligned} u(k) &= \Re\left\{y^*(k)e^{j(\phi+2\pi k\nu)}\right\}, \\ &= I(k)\cos(2\pi k\nu+\phi) + Q(k)\sin(2\pi k\nu+\phi), \quad (11)\\ v(k) &= \Im\left\{y^*(k)e^{j(\phi+2\pi k\nu)}\right\}, \\ &= I(k)\sin(2\pi k\nu+\phi) - Q(k)\cos(2\pi k\nu+\phi), \quad (12)\end{aligned}$$

[2]The actual modulation order is $M = 2^{2p}$ but we refer to it as p in this paper, for simplicity.

[3]Note that similar factorization was also used in [13] in the framework of NDA SNR estimation, but in the absence of the frequency offset. This new factorization approach is exploited differently in this paper in the presence of imperfect frequency synchronization.

and $F_{\boldsymbol{\theta}}(\cdot)$ is given by

$$F_{\boldsymbol{\theta}}(x) = \sum_{i=1}^{2^{p-1}}\exp\left\{-\frac{S^2(2i-1)^2d_p^2}{2\sigma^2}\right\}\cosh\left(\frac{2(2i-1)d_pSx}{\sigma^2}\right). \quad (13)$$

Then, injecting (10) in (6), it can be shown that $P[y(k);\boldsymbol{\theta}]$ can be factorized as follows:

$$P[y(k);\boldsymbol{\theta}] = \frac{4}{M\pi\sigma^2}\exp\left\{-\frac{I(k)^2+Q(k)^2}{\sigma^2}\right\} \times F_{\boldsymbol{\theta}}(u(k))F_{\boldsymbol{\theta}}(v(k)). \quad (14)$$

Moreover, since the transmitted symbols are assumed to be independent, then the corresponding AWGN-corrupted received samples are independent and the pdf of the received vector $\boldsymbol{y} = [y(k_0), y(k_0+1), \ldots, y(k_0+K-1)]$, parameterized by $\boldsymbol{\theta}$, is given by

$$P[\boldsymbol{y};\boldsymbol{\theta}] = \left(\frac{4}{M\pi\sigma^2}\right)^K\exp\left\{-\sum_{k=k_0}^{k_0+K-1}\frac{I(k)^2+Q(k)^2}{\sigma^2}\right\} \times \prod_{k=k_0}^{k_0+K-1}F_{\boldsymbol{\theta}}(u(k))F_{\boldsymbol{\theta}}(v(k)). \quad (15)$$

Finally, the log-likelihood function of the received vector is given by

$$\ln(P[\boldsymbol{y};\boldsymbol{\theta}]) = K\ln\left(\frac{4}{M\pi\sigma^2}\right) - \sum_{k=k_0}^{k_0+K-1}\frac{I(k)^2+Q(k)^2}{\sigma^2} + \sum_{k=k_0}^{k_0+K-1}\ln(F_{\boldsymbol{\theta}}(u(k))) + \sum_{k=k_0}^{k_0+K-1}\ln(F_{\boldsymbol{\theta}}(v(k))). \quad (16)$$

Therefore, due to the new factorization of the received samples pdf in (15), the log-likelihood function in (16) involves the sum of two analogous terms. This reduces the complexity of the derivation of its second partial derivatives and ultimately their expected values.

Then, we show that U_k and V_k (whose realizations are $u(k)$ and $v(k)$, respectively) are two independent and identically distributed random variables. This interesting property will be henceforth used to derive all the expectations. Indeed, exploiting the fact that $I(k)^2+Q(k)^2 = u(k)^2+v(k)^2$, it can be shown that $P[y(k);\boldsymbol{\theta}]$, given by (14), can be written as follows:

$$P[y(k);\boldsymbol{\theta}] = P[u(k);\boldsymbol{\theta}]P[v(k);\boldsymbol{\theta}] \quad (17)$$

where

$$P[u(k);\boldsymbol{\theta}] = \frac{2}{\sqrt{M\pi\sigma^2}}e^{-\frac{u(k)^2}{\sigma^2}}F_{\boldsymbol{\theta}}(u(k)) \quad (18)$$

$$P[v(k);\boldsymbol{\theta}] = \frac{2}{\sqrt{M\pi\sigma^2}}e^{-\frac{v(k)^2}{\sigma^2}}F_{\boldsymbol{\theta}}(v(k)). \quad (19)$$

Moreover, since $u(k) = \Re\{y(k)^*e^{j(2\pi k\nu+\phi)}\}$, $v(k) = \Im\{y(k)^*e^{j(2\pi k\nu+\phi)}\}$ and since $e^{j(2\pi k\nu+\phi)}$ is assumed to be deterministic, we have $P[y(k);\boldsymbol{\theta}] = P[u(k),v(k);\boldsymbol{\theta}]$ and therefore it follows from (17) that

$$P[u(k),v(k);\boldsymbol{\theta}] = P[u(k);\boldsymbol{\theta}]P[v(k);\boldsymbol{\theta}]. \tag{20}$$

Hence, the joint distribution of U_k and V_k is factorized into their elementary pdfs and, consequently, these are two independent random variables which are identically distributed according to (18) and (19).

Now, we partition the parameter vector $\boldsymbol{\theta} = [\nu\phi S\sigma^2]^T$ into two parameter vectors $\boldsymbol{\theta}^{(1)} = [\nu\phi]^T$ and $\boldsymbol{\theta}^{(2)} = [S\sigma^2]^T$, and we show that the FIM, $\boldsymbol{I}(\boldsymbol{\theta})$, is block-diagonal structured. In fact, it can be seen from (16) that averaging $(\partial^2\ln(P[\boldsymbol{y};\boldsymbol{\theta}])/\partial S\partial\nu)$ with respect to $P[\boldsymbol{y};\boldsymbol{\theta}]$ yields the following result:

$$\begin{aligned}\mathrm{E}_{\boldsymbol{Y}}\left\{\frac{\partial^2\ln(P[\boldsymbol{y};\boldsymbol{\theta}])}{\partial S\partial\nu}\right\} &= \sum_{k=k_0}^{k_0+K-1}\mathrm{E}_{Y_k}\left\{\frac{\partial^2\ln(F_\theta(u(k)))}{\partial S\partial\nu}\right\}\\ &\quad+\sum_{k=k_0}^{k_0+K-1}\mathrm{E}_{Y_k}\left\{\frac{\partial^2\ln(F_\theta(v(k)))}{\partial S\partial\nu}\right\}. \end{aligned}\tag{21}$$

In addition, we have

$$\frac{\partial\ln(F_{\boldsymbol{\theta}}(u(k)))}{\partial\nu} = -\frac{v(k)G_{\boldsymbol{\theta}}(u(k))}{F_{\boldsymbol{\theta}}(u(k))} \tag{22}$$

$$\frac{\partial\ln(F_{\boldsymbol{\theta}}(v(k)))}{\partial\nu} = \frac{u(k)G_{\boldsymbol{\theta}}(v(k))}{F_{\boldsymbol{\theta}}(v(k))} \tag{23}$$

where

$$\begin{aligned}G_{\boldsymbol{\theta}}(x) = 2\pi k\sum_{i=1}^{2^{p-1}}\frac{2S(2i-1)d_p}{\sigma^2}\exp\left\{-\frac{S^2(2i-1)^2d_p^2}{\sigma^2}\right\}\\ \times\sinh\left(\frac{2(2i-1)d_pSx}{\sigma^2}\right).\end{aligned}\tag{24}$$

We note also that averaging with respect to the univariate complex random variable Y_k is equivalent to averaging with respect to the bivariate real random variable (U_k,V_k), i.e., $\mathrm{E}_{Y_k}\{\,\cdot\,\} = \mathrm{E}_{(U_k,V_k)}\{\,\cdot\,\}$. Therefore, using these properties and injecting (22) and (23) in (21), we obtain the following result:

$$\begin{aligned}&\mathrm{E}_{\boldsymbol{Y}}\left\{\frac{\partial^2\ln(P[\boldsymbol{y};\boldsymbol{\theta}])}{\partial S\partial\nu}\right\}\\ &\quad=\sum_{k=k_0}^{k_0+K-1}\mathrm{E}_{U_k}\{u(k)\}\,\mathrm{E}_{V_k}\left\{\frac{\partial}{\partial S}\left(\frac{G_{\boldsymbol{\theta}}(v(k))}{F_{\boldsymbol{\theta}}(v(k))}\right)\right\}\\ &\quad-\sum_{k=k_0}^{k_0+K-1}\mathrm{E}_{V_k}\{v(k)\}\,\mathrm{E}_{U_k}\left\{\frac{\partial}{\partial S}\left(\frac{G_{\boldsymbol{\theta}}(u(k))}{F_{\boldsymbol{\theta}}(u(k))}\right)\right\}.\end{aligned}\tag{25}$$

Furthermore, it can be seen from (11) and (12) that[4] $\mathrm{E}_{U_k}\{u(k)\} = \mathrm{E}_{V_k}\{v(k)\} = 0$. Consequently, we obtain the following result:

$$\mathrm{E}_{\boldsymbol{Y}}\left\{\frac{\partial^2\ln(P[\boldsymbol{y};\boldsymbol{\theta}])}{\partial S\partial\nu}\right\} = 0. \tag{26}$$

More generally, we show that the expected values of the second derivatives with respect to an element of $\boldsymbol{\theta}^{(1)}$ and an element of $\boldsymbol{\theta}^{(2)}$ are all equal to zero. This can be formally written in the following succinct form:

$$\mathrm{E}_{\boldsymbol{Y}}\left\{\frac{\partial^2\ln(P[\boldsymbol{y};\boldsymbol{\theta}])}{\partial\theta_i^{(1)}\partial\theta_j^{(2)}}\right\} = 0, i,j = 1,2. \tag{27}$$

Thus, the FIM associated with the square QAM modulated signals has a block diagonal structure:

$$\boldsymbol{I}(\boldsymbol{\theta}) = \begin{pmatrix}\boldsymbol{I}^{(1)}(\boldsymbol{\theta}) & \mathbf{0}\\ \mathbf{0} & \boldsymbol{I}^{(2)}(\boldsymbol{\theta})\end{pmatrix} \tag{28}$$

where $\boldsymbol{I}^{(1)}(\boldsymbol{\theta})$ is the FIM pertaining to the NDA estimates of the carrier frequency and phase offsets, and $\boldsymbol{I}^{(2)}(\boldsymbol{\theta})$ is the FIM associated with the unknown nuisance parameters. Due to the block diagonal structure of the global FIM, $\boldsymbol{I}(\boldsymbol{\theta})$, the two parameter vectors $\boldsymbol{\theta}^{(1)}$ and $\boldsymbol{\theta}^{(2)}$ are decoupled. Hence, we prove here, for the first time, over QAM transmissions, that we deal with two separate problems regarding the estimation of the synchronization parameters on one hand and the estimation of the signal amplitude and the noise power on the other. Therefore, the NDA CRLBs of the phase and frequency estimates (which correspond to the first and the second diagonal elements of $\boldsymbol{I}^{-1}(\boldsymbol{\theta})$) do not involve the elements of $\boldsymbol{I}^{(2)}(\boldsymbol{\theta})$. Hence, we conclude that rendering the signal amplitude and the noise power unknown does not affect the ultimate estimation error of the synchronization parameters. Therefore, the existing synchronization algorithms that were derived assuming the perfect knowledge of these two nuisance parameters (S and σ^2) will ultimately exhibit the same performance, in practical scenarios where their perfect estimation/knowledge is much easier said than done. Moreover, although the block diagonal structure of the global FIM allows the derivation of the frequency and phase NDA CRLBs, even without deriving $\boldsymbol{I}^{(2)}(\boldsymbol{\theta})$, we refer the reader to [13] for the expression of $\boldsymbol{I}^{(2)}(\boldsymbol{\theta})$ which was derived in the framework of SNR estimation. Thus, in the sequel, we will only derive the elements of the matrix $\boldsymbol{I}^{(1)}(\boldsymbol{\theta})$ which allows the derivation of the CRLBs for the synchronization parameters of interest. To that end, we will only detail the derivation of the first diagonal element of $\boldsymbol{I}^{(1)}(\boldsymbol{\theta})$, for the sake of briefness, and the derivation of its remaining entries follows readily in the same way. In fact, since U_k and V_k are identically distributed, it can be shown that

$$\mathrm{E}_{\boldsymbol{Y}}\left\{\frac{\partial^2\ln(P[\boldsymbol{y};\boldsymbol{\theta}])}{\partial\nu^2}\right\} = 2\sum_{k=k_0}^{k_0+K-1}\mathrm{E}_{Y_k}\left\{\frac{\partial^2\ln(F_{\boldsymbol{\theta}}(u(k)))}{\partial\nu^2}\right\}. \tag{29}$$

To derive the expression of $\mathrm{E}_{Y_k}\left\{\partial^2\ln(F_{\boldsymbol{\theta}}(u(k)))/\partial\nu^2\right\}$, we need to derive the second derivative of $F_{\boldsymbol{\theta}}(u(k))$ with respect to ν as follows:

$$\frac{\partial^2F_{\boldsymbol{\theta}}(u(k))}{\partial\nu^2} = v(k)^2R_{\boldsymbol{\theta}}(u(k)) - 2\pi ku(k)G_{\boldsymbol{\theta}}(u(k)) \tag{30}$$

where $G_{\boldsymbol{\theta}}(\,\cdot\,)$ is given by (24) and $R_{\boldsymbol{\theta}}(\,\cdot\,)$ is defined as

$$\begin{aligned}R_{\boldsymbol{\theta}}(x) = (2\pi)^2k^2\sum_{i=1}^{2^{p-1}}\frac{4S^2(2i-1)^2d_p^2}{\sigma^4}\\ \times\exp\left\{-\frac{S^2(2i-1)^2d_p^2}{\sigma^2}\right\}\cosh\left(\frac{2(2i-1)d_pSx}{\sigma^2}\right).\end{aligned}\tag{31}$$

[4]This is because the transmitted symbols are assumed equally likely drawn from a symmetric constellation and the noise is zero-mean. This implies that $\mathrm{E}\{I(k)\} = \mathrm{E}\{Q(k)\} = 0$.

Hence, straightforward algebraic manipulations yield the following result:

$$\frac{\partial^2 \ln(F_{\boldsymbol{\theta}}(u(k)))}{\partial \nu^2} = -2\pi k u(k) \frac{G_{\boldsymbol{\theta}}(u(k))}{F_{\boldsymbol{\theta}}(u(k))} + v(k)^2 \left[\frac{R_{\boldsymbol{\theta}}(u(k))}{F_{\boldsymbol{\theta}}(u(k))} - \left(\frac{G_{\boldsymbol{\theta}}(u(k))}{F_{\boldsymbol{\theta}}(u(k))} \right)^2 \right]. \quad (32)$$

Next, for convenience, we will use the following ones:

$$H_{\boldsymbol{\theta}}(u(k)) = \frac{G_{\boldsymbol{\theta}}(u(k))}{F_{\boldsymbol{\theta}}(u(k))} \quad (33)$$

$$K_{\boldsymbol{\theta}}(u(k)) = \frac{R_{\boldsymbol{\theta}}(u(k))}{F_{\boldsymbol{\theta}}(u(k))}. \quad (34)$$

Thus, averaging (32) with respect to Y_k and using the fact that U_k and V_k are independent, we obtain

$$\begin{aligned} &\mathrm{E}_{Y_k}\left\{ \frac{\partial^2 \ln(F_{\boldsymbol{\theta}}(u(k)))}{\partial \nu^2} \right\} \\ &\quad = -2\pi k \mathrm{E}_{U_k}\left\{ u(k) H_{\boldsymbol{\theta}}(u(k)) \right\} \\ &\qquad + \mathrm{E}_{V_k}\left\{ v(k)^2 \right\} \left(\mathrm{E}_{U_k}\left\{ K_{\boldsymbol{\theta}}(u(k)) \right\} - \mathrm{E}_{U_k}\left\{ H_{\boldsymbol{\theta}}(u(k))^2 \right\} \right). \end{aligned} \quad (35)$$

After deriving the different expectations involved in (35), as detailed in Appendix B, we obtain the final expression of the first diagonal element of $\boldsymbol{I}^{(1)}(\boldsymbol{\theta})$ as follows:

$$\mathrm{E}_{\boldsymbol{Y}}\left\{ \frac{\partial^2 \ln(P[\boldsymbol{y};\boldsymbol{\theta}])}{\partial \nu^2} \right\} = (2\pi)^2 2\rho \left(\rho - \frac{(1+\rho)}{A_2} \Psi(\rho) \right) \sum_{k=k_0}^{k_0+K-1} k^2 \quad (36)$$

where A_2 and $\Psi(\cdot)$ are defined as

$$A_2 = \sum_{i=1}^{2^{p-1}} (2i-1)^2 \quad (37)$$

$$\Psi(\rho) = \frac{1}{\sqrt{2\pi}} \int_{-\infty}^{+\infty} \frac{f_\rho^2(t)}{\delta_\rho(t)} e^{-\frac{t^2}{2}} dt \quad (38)$$

with

$$f_\rho(t) = \sum_{i=1}^{2^{p-1}} (2i-1) e^{-(2i-1)^2 d_p^2 \rho} \sinh\left(\sqrt{2\rho}(2i-1) d_p t \right) \quad (39)$$

$$\delta_\rho(t) = \sum_{i=1}^{2^{p-1}} e^{-(2i-1)^2 d_p^2 \rho} \cosh\left((2i-1) d_p \sqrt{2\rho} t \right). \quad (40)$$

Then, using equivalent manipulations to derive the other elements of $\boldsymbol{I}^{(1)}(\boldsymbol{\theta})$, we obtain the following result:

$$\boldsymbol{I}^{(1)}(\boldsymbol{\theta}) = 2\rho \left(\rho - \frac{(1+\rho)}{A_2} \Psi(\rho) \right) \times \begin{pmatrix} (2\pi)^2 \sum_{k=k_0}^{k_0+K-1} k^2 & 2\pi \sum_{k=k_0}^{k_0+K-1} k \\ 2\pi \sum_{k=k_0}^{k_0+K-1} k & K \end{pmatrix}. \quad (41)$$

We notice from (41) that the FIM associated with the synchronization parameters, $\boldsymbol{I}^{(1)}(\boldsymbol{\theta})$, depends on the time index k_0. Hence, we have different loose bounds as k_0 varies. We are interested in the tightest (highest) bound which can be shown to be achieved by choosing k_0 in the middle of the observation interval. Hence, when the joint estimator is analyzed relative to the middle of the observation interval (i.e., $k_0 = -(K-1)/2$), $\boldsymbol{I}^{(1)}(\boldsymbol{\theta})$ becomes diagonal and the frequency and phase parameters are decoupled. In this case, after inverting $\boldsymbol{I}(\boldsymbol{\theta})$, we obtain the closed-form expressions for the CRLBs of the joint estimation of the parameters ν, ϕ as follows:

$$\mathrm{CRLB}(\nu) = \frac{-6}{(2\pi)^2 K(K^2-1)\rho \left(\rho - \frac{(1+\rho)\Psi(\rho)}{A_2} \right)} \quad (42)$$

$$= \left(\frac{-1}{\rho - \frac{(1+\rho)}{A_2}\Psi(\rho)} \right) \mathrm{MCRLB}(\nu). \quad (43)$$

$$\mathrm{CRLB}(\phi) = \frac{-1}{2K\rho \left(\rho - \frac{(1+\rho)\Psi(\rho)}{A_2} \right)} \quad (44)$$

$$= \left(\frac{-1}{\rho - \frac{(1+\rho)}{A_2}\Psi(\rho)} \right) \mathrm{MCRLB}(\phi). \quad (45)$$

Note that the expressions of the MCRLBs of the frequency and phase estimates given by

$$\mathrm{MCRLB}(\nu) = \frac{6}{(2\pi)^2 K(K^2-1)\rho} \quad (46)$$

$$\mathrm{MCRLB}(\phi) = \frac{1}{2K\rho} \quad (47)$$

were earlier derived in [8] for any linearly-modulated signal assuming the signal amplitude and the noise to be perfectly known. We emphasize, however, that these expressions are also applicable in our model where we assume the signal amplitude and the noise power to be unknown nuisance parameters. Indeed, as warranted by the block-diagonal structure of the FIM in (28), these two parameters are decoupled from the unknown phase and frequency.

We also mention that the newly derived expressions in (42) to (45) allow the immediate evaluation of the frequency and phase CRLBs, contrarily to the very complex approach earlier introduced in [9]. Besides, we note from (43) and (45) that the CRLBs of the carrier frequency and the carrier phase are proportional to their MCRLBs within the same factor $-1/\rho - (1+\rho)/A_2\Psi(\rho)$. This means that rendering the symbols completely unknown affects the ultimate estimation accuracy of these two parameters in the same way. We note also that this common factor depends only on the modulation order and the SNR. In the next section, this factor will be shown by simulations to converge asymptotically to 1 versus the SNR, regardless of the modulation order, thereby confirming that the MCRLB is a good approximation of the CRLB at high SNRs.

Finally, it is worth noting that the analytical expressions for the CRLBs as a function of the true SNR, established in (42) to (45), generalize the elegant CRLB expressions derived in [11] for a QPSK constellation to higher-order square QAM modulations. In fact, it can be verified that the closed-form expressions

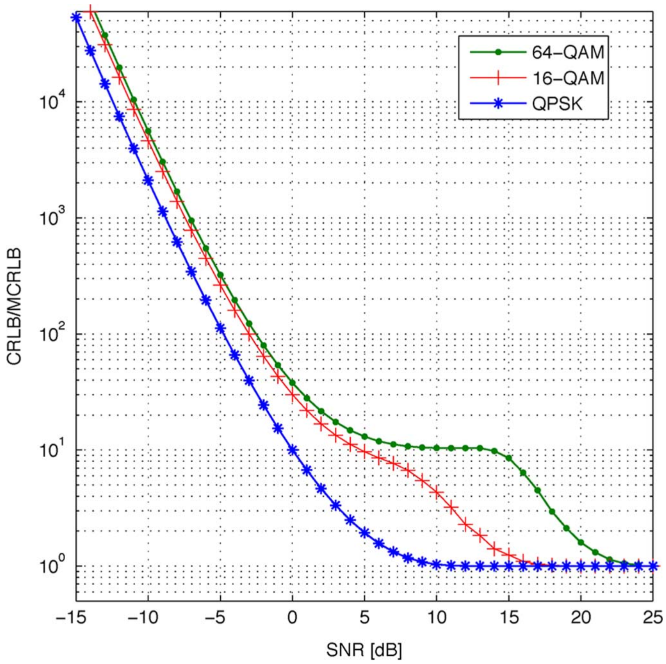

Fig. 1. CRLB(ν)/MCRLB(ν) = CRLB(ϕ)/MCRLB(ϕ) versus SNR.

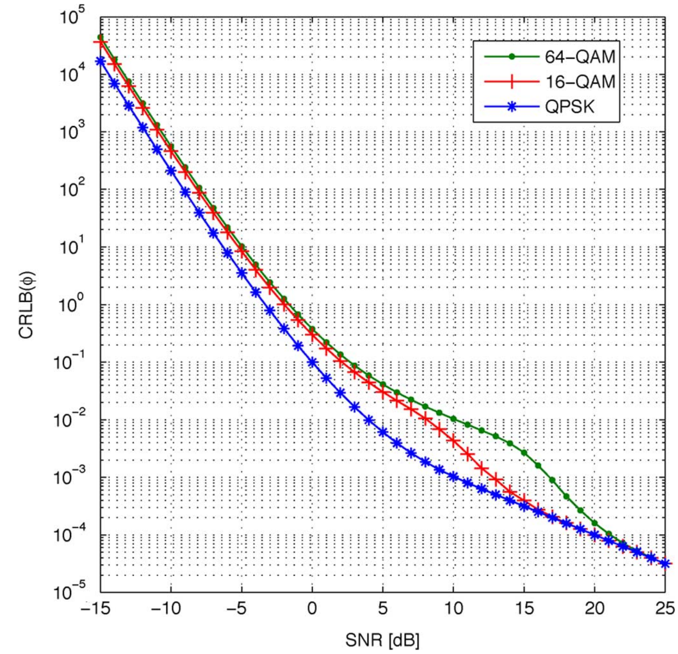

Fig. 2. CRLB(ϕ) versus SNR when $K = 100$.

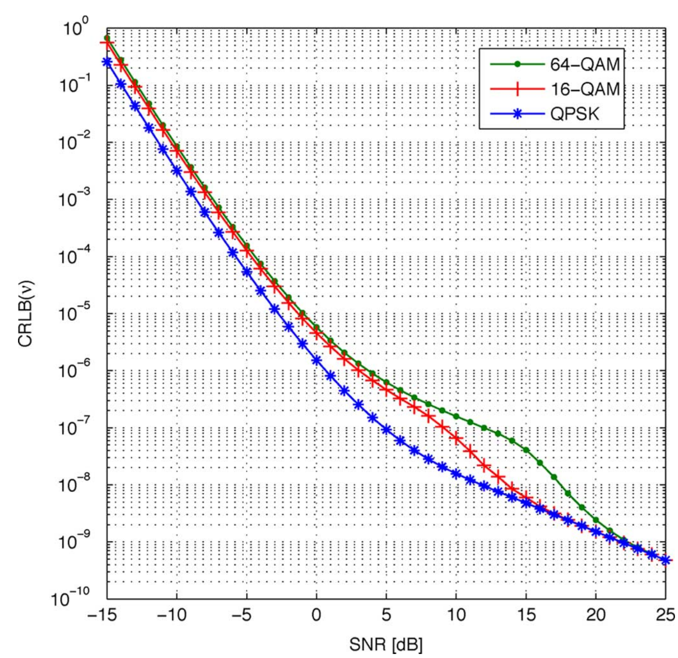

Fig. 3. CRLB(ν) versus SNR when $K = 100$.

of the FIM derived in [11, eqs. (3)–(6)] for QPSK signals correspond to the special case of $p = 1$ in the general expressions derived in this paper.

IV. Graphical Representations

In this section, for different modulation orders and for each parameter, we provide graphical representations of the CRLB to the MCRLB ratio[5] in Fig. 1 and of the CRLBs in Figs. 2 and 3. The window observation size is set to $K = 100$.

Beforehand, we note that the even integrand function $f_\rho^2(t)/\delta_\rho(t)$ involved in (38) takes extremely small values as $|t|$ increases. Its integral over $[-\infty, +\infty]$ can be therefore accurately approximated by a finite integral over a finite support $[-T, T]$, for which the Riemann integration method (simple summation) can be adequately used. In our simulations, it should be noted that $T = 100$ and a summation step of 1 provided very accurate values for the infinite integral and that the CRLB curves obtained in this paper are identical to those previously presented in [9]. In fact, as shown in Fig. 1, it can be verified that our analytical expressions for the CRLB to the MCRLB ratios and their numerical and empirical values computed previously in ([9], Fig. 2) are in very good agreement for the considered constellations (QPSK, 16-QAM and 64-QAM signals).

Moreover, from Fig. 1, we notice that at low SNR values the MCRLB is a looser bound compared to the true CRLB. In fact, for relatively large observation window sizes ($K = 100$ in our case), the MCRLB almost equals the DA CRLB (known data sequence), which is itself known to be smaller than the NDA CRLB (unknown data sequence). Whereas at high SNR values, we notice that the MCRLB is tightly close to the CRLB as their ratio converges asymptotically to 1. Consequently, as the CRLBs and the MCRLBs coincide in this SNR region, it is more interesting to use the latter as a benchmark to evaluate the performance of unbiased estimators at high SNR values. As depicted in Figs. 2 to 3, we notice indeed that the CRLBs for different modulation orders coincide at high SNR values, as the MCRLBs themselves do not depend on the modulation order, as shown in (46)–(47).

V. Conclusion

In this paper, we derived for the first time the analytical expressions of the NDA CRLBs of the carrier frequency and phase offsets from square QAM signals. The signal and noise powers were considered as unknown nuisance parameters and

[5]As seen from (43) and (45), the ratio of the CRLB to the MCRLB is the same for the phase and the frequency and is hence plotted in Fig. 1 for both.

we confirmed that their perfect knowledge does not bring any additional information regarding the estimation of the considered synchronization parameters. These lower bounds serve as benchmarks for the achievable performance of actual unbiased estimators. We confirmed that the MCRLB is a good approximation of the true CRLB in the high-SNR region. Therefore, using the MCRLB in this SNR region is more interesting since it is simpler to evaluate. Furthermore, we showed that the frequency and the phase CRLBs computed using our analytical expressions are identical to those computed empirically or numerically in [9]. Finally, our proposed analytical expressions coincide with those recently derived in closed-form, but only for QPSK signals [11], thereby providing an elegant generalization to arbitrary square QAM-modulated transmissions, so timely for the understanding of fundamental limits on the estimation accuracy of key channel parameters in today's and future high-data-rate transmission applications.

APPENDIX A
PROOF OF THE FACTORIZATION OF $D_{\boldsymbol{\theta}}(k)$ IN (10)

Denoting by $\tilde{\mathcal{C}}$ the subset of the alphabet points that lie in the top-right quadrant of the constellation, i.e., $\tilde{\mathcal{C}} = \{(2i-1)d_p + j(2m-1)d_p\}_{i,m=1,2,\ldots,2^{p-1}}$, we have $\mathcal{C} = \tilde{\mathcal{C}} \cup (-\tilde{\mathcal{C}}) \cup \tilde{\mathcal{C}}^* \cup (-\tilde{\mathcal{C}}^*)$ and we rewrite (7) as follows:

$$\begin{aligned}D_{\boldsymbol{\theta}}(k) = \sum_{\tilde{c}_l \in \tilde{\mathcal{C}}} \exp\left\{-\frac{S^2|\tilde{c}_l|^2}{\sigma^2}\right\} \\ \times \left[\exp\left\{\frac{2S\Re\left\{y^*(k)e^{j(\phi+2\pi k\nu)}\tilde{c}_l\right\}}{\sigma^2}\right\}\right. \\ +\exp\left\{\frac{2S\Re\left\{y^*(k)e^{j(\phi+2\pi k\nu)}(-\tilde{c}_l)\right\}}{\sigma^2}\right\} \\ +\exp\left\{\frac{2S\Re\left\{y^*(k)e^{j(\phi+2\pi k\nu)}\tilde{c}_l^*\right\}}{\sigma^2}\right\} \\ \left.+\exp\left\{\frac{2S\Re\left\{y^*(k)e^{j(\phi+2\pi k\nu)}(-\tilde{c}_l^*)\right\}}{\sigma^2}\right\}\right]. \quad (48)\end{aligned}$$

Then using the fact that $e^x + e^{-x} = 2\cosh(x)$, we obtain

$$\begin{aligned}D_{\boldsymbol{\theta}}(k) = 2\sum_{\tilde{c}_l \in \tilde{\mathcal{C}}} \exp\left\{-\frac{S^2|\tilde{c}_l|^2}{\sigma^2}\right\} \\ \times \left[\cosh\left(\frac{2S\Re\left\{y^*(k)e^{j(\phi+2\pi k\nu)}\tilde{c}_l\right\}}{\sigma^2}\right)\right. \\ \left.+\cosh\left(\frac{2S\Re\left\{y^*(k)e^{j(\phi+2\pi k\nu)}\tilde{c}_l{}^*\right\}}{\sigma^2}\right)\right]. \quad (49)\end{aligned}$$

Moreover, we have $\cosh(x) + \cosh(y) = 2\cosh(x+y/2)\cosh(x-y/2)$, and using the fact that $\tilde{c}_l + \tilde{c}_l^* = 2\Re\{\tilde{c}_l\}$ and $\tilde{c}_l - \tilde{c}_l^* = 2j\Im\{\tilde{c}_l\}$, (49) is rewritten as follows:

$$\begin{aligned}D_{\boldsymbol{\theta}}(k) = 4\sum_{\tilde{c}_l \in \tilde{\mathcal{C}}} \exp\left\{-\frac{S^2|\tilde{c}_l|^2}{\sigma^2}\right\} \\ \times \cosh\left(\frac{2S\Re\{\tilde{c}_l\}\Re\left\{y^*(k)e^{j(\phi+2\pi k\nu)}\right\}}{\sigma^2}\right) \\ \times \cosh\left(\frac{2S\Im\{\tilde{c}_l\}\Im\left\{y^*(k)e^{(j\phi+2\pi k\nu)}\right\}}{\sigma^2}\right). \quad (50)\end{aligned}$$

Now using the fact that $\tilde{\mathcal{C}} = \{(2i-1)d_p + j(2m-1)d_p\}_{i,m=1,2,\ldots,2^{p-1}}$, the term $D_{\boldsymbol{\theta}}(k)$ is rewritten as follows:

$$\begin{aligned}D_{\boldsymbol{\theta}}(k) \\ = 4\sum_{i=1}^{2^{p-1}}\sum_{m=1}^{2^{p-1}} \exp\left\{-\frac{S^2((2i-1)^2+(2m-1)^2)d_p^2}{\sigma^2}\right\} \\ \times \cosh\left(\frac{2S(2i-1)d_p\Re\left\{y^*(k)e^{j(\phi+2\pi k\nu)}\right\}}{\sigma^2}\right) \\ \times \cosh\left(\frac{2S(2m-1)d_p\Im\left\{y^*(k)e^{j(\phi+2\pi k\nu)}\right\}}{\sigma^2}\right). \quad (51)\end{aligned}$$

Finally, splitting the two sums in (51), it can be shown that $D_{\boldsymbol{\theta}}(k)$ is factorized as follows:

$$D_{\boldsymbol{\theta}}(k) = 4F_{\boldsymbol{\theta}}(u(k)) \times F_{\boldsymbol{\theta}}(v(k)) \quad (52)$$

where $u(k)$ and $v(k)$ and $F_{\boldsymbol{\theta}}(\cdot)$ are defined in (11), (12), and (13), respectively.

APPENDIX B
PROOF OF (36)

We have

$$\begin{aligned}\mathrm{E}_{V_k}\left\{v(k)^2\right\} \\ = \int_{-\infty}^{+\infty} v(k)^2 P[v(k);\boldsymbol{\theta}]dv(k), \\ = \frac{2}{\sqrt{M\pi\sigma^2}}\int_{-\infty}^{+\infty} v(k)^2 e^{-\frac{v(k)^2}{\sigma^2}} F_{\boldsymbol{\theta}}(v(k))dv(k), \\ = \frac{2}{\sqrt{M\pi\sigma^2}}\sum_{i=1}^{2^{p-1}} \sqrt{\pi}\sigma\left(\frac{\sigma^2}{2} + S^2(2i-1)^2 d_p^2\right). \quad (53)\end{aligned}$$

Recall that $M = 2^{2p}$, and hence we obtain

$$\mathrm{E}_{V_k}\left\{v(k)^2\right\} = \frac{\sigma^2}{2} + \frac{S^2 d_p^2}{2^{p-1}}\sum_{i=1}^{2^{p-1}}(2i-1)^2 = \frac{1}{2}(\sigma^2+S^2). \quad (54)$$

Likewise, averaging with respect to $P[u(k);\boldsymbol{\theta}]$ given by (18) and inverting the sum and the integral signs, we are able to derive $\mathrm{E}_{U_k}\left\{u(k)H_{\boldsymbol{\theta}}(u(k))\right\}$, $\mathrm{E}_{U_k}\left\{K_{\boldsymbol{\theta}}(u(k))\right\}$ and $\mathrm{E}_{U_k}\left\{H_{\boldsymbol{\theta}}(u(k))^2\right\}$ as follows:

$$\begin{aligned}
&\mathrm{E}_{U_k}\left\{u(k)H_{\boldsymbol{\theta}}(u(k))\right\}\\
&= \frac{2}{\sqrt{M\pi\sigma^2}}\int_{-\infty}^{+\infty} u(k)G_{\boldsymbol{\theta}}(u(k))e^{-\frac{u(k)^2}{\sigma^2}}du(k),\\
&= \frac{2\pi k}{2^{p-1}}\frac{2S^2d_p^2}{\sigma^2}\sum_{i=1}^{2^{p-1}}(2i-1)^2,\\
&= 2\pi k\rho, \qquad (55)\\
&\mathrm{E}_{U_k}\left\{K_{\boldsymbol{\theta}}(u(k))\right\}\\
&= \frac{2}{\sqrt{M\pi\sigma^2}}\int_{-\infty}^{+\infty} R_{\boldsymbol{\theta}}(u(k))e^{-\frac{u(k)^2}{\sigma^2}}du(k),\\
&= \frac{(2\pi)^2k^2}{2^{p-1}}\frac{4S^2d_p^2}{\sigma^4}\sum_{i=1}^{2^{p-1}}(2i-1)^2,\\
&= 2(2\pi)^2k^2\frac{\rho}{\sigma^2}, \qquad (56)\\
&\mathrm{E}_{U_k}\left\{H_{\boldsymbol{\theta}}(u(k))^2\right\}\\
&= \frac{2}{\sqrt{M\pi\sigma^2}}\int_{-\infty}^{+\infty} \frac{G_{\boldsymbol{\theta}}^2(u(k))}{F_{\boldsymbol{\theta}}(u(k))}e^{-\frac{u(k)^2}{\sigma^2}}du(k). \qquad (57)
\end{aligned}$$

We simplify (57) by changing $u(k)/\sigma$ by t and we obtain the following result:

$$\mathrm{E}_{U_k}\left\{H_{\boldsymbol{\theta}}(u(k))^2\right\} = 2(2\pi)^2k^2\frac{\rho}{\sigma^2A_2}\Psi(\rho) \qquad (58)$$

where A_2 and $\Psi(\cdot)$ are defined in (37) and (38) respectively. Then we inject (54), (55), (56) and (58) into (35) and we obtain:

$$\mathrm{E}_{Y_k}\left\{\frac{\partial^2 \ln(F_{\boldsymbol{\theta}}(u(k))}{\partial\nu^2}\right\} = (2\pi)^2k^2\rho\left(\rho - \frac{(1+\rho)}{A_2}\Psi(\rho)\right). \qquad (59)$$

Finally, plugging (59) into (29), the first diagonal element of $\boldsymbol{I}^{(1)}(\boldsymbol{\theta})$ follows immediately as

$$\mathrm{E}_{\boldsymbol{Y}}\left\{\frac{\partial^2 \ln(P[\boldsymbol{y};\boldsymbol{\theta}])}{\partial\nu^2}\right\} = (2\pi)^2 2\rho\left(\rho - \frac{(1+\rho)}{A_2}\Psi(\rho)\right)\sum_{k=k_0}^{k_0+K-1}k^2. \qquad (60)$$

REFERENCES

[1] F. Bellili, N. Atitallah, S. Affes, and A. Stéphenne, "Closed-form expressions for the exact Cramér–Rao bound for parameter estimation of arbitrary square QAM-modulated signals," presented at the IEEE GLOBECOM, Honolulu, HI, Nov.–Dec. 2009.

[2] U. Mengali and M. Morelli, "Data-aided frequency estimation for burst digital transmission," *IEEE Trans. Commun.*, vol. 45, no. 1, pp. 23–25, Jan. 1997.

[3] K. V. Cartwright, "Blind phase recovery in cross QAM communication systems with eighth-order statistics," *IEEE Signal Process. Lett.*, vol. 8, no. 12, pp. 304–306, Dec. 2001.

[4] P. Campisi, G. Panci, S. Colonnese, and G. Scarano, "Blind phase recovery for QAM communication systems," *IEEE Trans. Signal Process.*, vol. 53, no. 4, pp. 1348–1358, Apr. 2005.

[5] M. Moeneclaey, "On the true and the modified Cramér–Rao bounds for the estimation of a scalar parameter in the presence of nuisance parameters," *IEEE Trans. Commun.*, vol. 46, no. 11, pp. 1536–1544, Nov. 1998.

[6] H. Steendam and M. Moeneclaey, "Low SNR limit of the Cramér–Rao bound for estimating the carrier phase and frequency of a PAM, PSK, or QAM waveform," *IEEE Commun. Lett.*, vol. 5, no. 5, pp. 215–217, May 2001.

[7] A. N. D'Andrea, U. Mengali, and R. Reggiannini, "The modified Cramér–Rao bound and its application to synchronization parameters," *IEEE J. Sel. Areas Commun.*, vol. 42, no. 2/3/4, pp. 1391–1399, Apr. 1994.

[8] F. Gini, R. Reggiannini, and U. Mengali, "The modified Cramér–Rao bound in vector parameter estimation," *IEEE Trans. Commun.*, vol. 46, no. 1, pp. 52–60, Jan. 1998.

[9] B. Cowley, F. Rice, and M. Rice, "Cramér–Rao lower bound for QAM phase and frequency estimation," *IEEE Trans. Commun.*, vol. 49, no. 9, pp. 689–693, Sep. 2001.

[10] N. Noels, H. Steendam, and M. Moeneclaey, "The true Cramér–Rao bound for carrier frequency estimation from a PSK signal," *IEEE Trans. Commun.*, vol. 52, no. 5, pp. 834–844, May 2004.

[11] J. P. Delmas, "Closed form-expressions of the exact Cramér–Rao bound for parameter estimation of BPSK, MSK, or QPSK waveforms," *IEEE Signal Process. Lett.*, vol. 15, pp. 405–408, Apr. 2008.

[12] S. M. Kay, *Fundamentals of Statistical Signal Processing, Vol. 1: Estimation Theory*. Upper Saddle River, NJ: Prentice-Hall, 1993.

[13] F. Bellili, A. Stéphenne, and S. Affes, "Cramér–Rao bound for NDA SNR estimates of square QAM-modulated transmissions," *IEEE Trans. Commun.*, Oct. 2008, submitted for publication.

Faouzi Bellili was born in Sbeitla, Kasserine, Tunisia, on June 16, 1983. He received the Diplôme d'Ingénieur in Signals and Systems (with Hons.) from the Tunisia Polytechnic School in 2007 and the M.Sc. degree, with exceptional grade, at the Institut National de la Recherche Scientifique-Énergie, Matériaux, et Télécommunications (INRS-ÉMT), Université du Québec, Montréal, QC, Canada, in 2009. He is currently working towards the Ph.D. degree at INRS-EMT.

His research focuses on statistical signal processing and array processing with an emphasis on parameters estimation for wireless communications. While pursuing the M.Sc. degree, he authored/coauthered six international journal papers and more than ten international conference papers.

Mr. Bellili has been selected by INRS as its candidate for the 2009–2010 competition of the very prestigious Vanier Canada Graduate Scholarships program. He acts regularly as a reviewer for many international scientific journals and conferences. He is the recipient of the National grant of excellence from the Tunisian Government.

Nesrine Atitallah received the Diplôme d'Ingénieur in Signals and Systems (with Hons.) from the Tunisia Polytechnic School in 2009. She is now working towards the M.Sc. degree in electrical engineering at the Tunisia Polytechnic School.

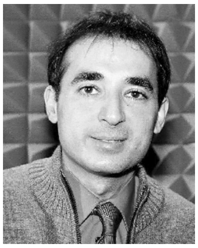

Sofiène Affes (S'94–M'95–SM'04) received the Diplôme d'Ingénieur degree in electrical engineering and the Ph.D. degree (with Hons.) in signal processing, both from the École Nationale Supérieure des Télécommunications (ENST), Paris, France, in 1992 and 1995, respectively.

From 1995 until 1997, he was a Research Associate and from 1997 until 2000 an Assistant Professor with the INRS-EMT, University of Quebec, Montreal, QC, Canada. Currently, he is an Associate Professor in the Wireless Communications Group. His research interests are in wireless communications, statistical signal and array processing, adaptive space-time processing, and MIMO. From 1998 to 2002, he has been leading the radio design and signal processing activities of the Bell/Nortel/NSERC Industrial Research Chair in Personal Communications at INRS-EMT, Montreal, QC, Canada. Since 2004, he has been actively involved in major projects in wireless of PROMPT (Partnerships for Research on Microelectronics, Photonics and Telecommunications).

Prof. Affes was the corecipient of the 2002 Prize for Research Excellence of INRS. He currently holds a Canada Research Chair in Wireless Communications and a Discovery Accelerator Supplement Award from NSERC (Natural Sciences & Engineering Research Council of Canada). In 2006, he served as a General Co-Chair of the IEEE Vehicular Technology Conference (VTC) 2006—Fall, Montreal, QC, Canada. In 2008, he received from the IEEE Vehicular Technology Society the IEEE VTC Chair Recognition Award for exemplary contributions to the success of IEEE VTC. He currently acts as a member of the Editorial Board of the IEEE TRANSACTIONS ON WIRELESS COMMUNICATIONS and of the Wiley *Journal on Wireless Communications & Mobile Computing*.

Alex Stéphenne (M'95–SM'96) was born in Quebec, Canada, on May 8, 1969. He received the B.Ing. degree in electrical engineering from McGill University, Montreal, QC, Canada, in 1992 and the M.Sc. and Ph.D. degrees in telecommunications from the INRS-Télécommunications, Université du Québec, Montreal, QC, Canada in 1994 and 2000, respectively.

In 1999 he joined SITA Inc., Montreal, QC, Canada, where he worked on the design of remote management strategies for the computer systems of airline companies. In 2000, he became a DSP Design Specialist for Dataradio Inc., Montreal, QC, Canada, a company specializing in the design and manufacturing of advanced wireless data products and systems for mission critical applications. In January 2001, he joined Ericsson and worked for over two years in Sweden, where he was responsible for the design of baseband algorithms for WCDMA commercial base station receivers. From June 2003 to December 2008, he continued working for Ericsson, but based in Montreal, where he was a researcher focusing on issues related to the physical layer of wireless communication systems. Currently, he is with Huawei Technologies Canada, Ottawa, ON, Canada. He is also an Adjunct Professor at INRS. His current research interests include wireless channel modeling/characterization/estimation as well as statistical signal processing, array processing, and adaptive filtering for wireless telecommunication applications.

Dr. Stéphenne is a member of the Ordre des Ingénieurs du Québec. He has served as a Co-Chair for the Multiple Antenna Systems and Space-Time Processing track of the 2008—Fall IEEE Vehicular Technology Conference (VTC'08-Fall) in Calgary, AB, Canada, as a Co-Chair of the Technical Program Committee (TPC) for VTC'06-Fall, Montreal, QC, Canada, and as a TPC member for VTC'05-Fall, Stockholm, Sweden. He acts regularly as a reviewer for many international scientific journals and conferences and for the funding organizations NSERC.